

AMES-HET 99-06

UCRHEP-T258

BNL-HET-99/13

Gauge Boson – Gauge Boson Scattering in Theories with Large Extra Dimensions

David Atwood¹

Department of Physics and Astronomy, Iowa State University, Ames, IA 50011

Shaouly Bar-Shalom²

Department of Physics, University of California, Riverside, CA 92521

and

Amarjit Soni³

Theory Group, Brookhaven National Laboratory, Upton, NY 11973

Abstract:

We consider the scattering amplitudes of the form $V_1 V_2 \rightarrow V_3 V_4$, where $V_i = \gamma, Z, W$ or g (=gluon) are the Standard Model gauge bosons, due to graviton exchange in Kaluza-Klein theories with large extra dimensions. This leads to a number of experimentally viable signatures at high energy leptonic and hadronic colliders. We discuss the observability or attainable limits on the scale of the gravitational interactions (m_D), that may be obtained at an e^+e^- Next Linear Collider (NLC) and at the LHC, by studying some of these type of gauge boson scattering processes. We find that the attainable limits through these type of processes are: $m_D \gtrsim 3$ TeV at the NLC and $m_D \gtrsim 6$ TeV at the LHC.

¹email: atwood@iastate.edu

²email: shaouly@phyun0.ucr.edu

³email: soni@bnl.gov

1 Introduction

Although gravity is the weakest force in nature and naive dimensional arguments suggest that its effect on high energy collisions is insignificant below energies of the Planck scale $M_P = G_N^{-1/2} = 1.22 \times 10^{19} \text{ GeV}$, recent advances in M-theory [1] have motivated the consideration of Kaluza-Klein theories which allow gravitational interactions to become strong at relatively modest energies compared to the Planck scale, perhaps as low as 1 TeV [2, 3].

M-theory is a special case of Kaluza-Klein theories where there are total of 11 dimensions. Four of these are of course the usual space time while the other 7 are compact. The possibility which emerges from [2, 3] is that while some of the compact dimensions have lengths near the Planck scale, n of these dimensions may be compactified with a distance scale R which is much larger. This leads to an effective Planck mass m_D , perhaps of the order of 1 TeV which is related to the size R of the new dimension according to [2]:

$$8\pi R^n m_D^{2+n} \sim M_P^2 . \quad (1)$$

In this scenario, at distances $d < R$ the Newtonian inverse square law will fail [2]. If $n = 1$ and $m_D = 1 \text{ TeV}$, then R is of the order of 10^8 km , large on the scale of the solar system, which is clearly ruled out by astronomical observations. However, if $n \geq 2$ then $R < 1 \text{ mm}$; there are no experimental constraints on the behavior of gravitation at such scales [4] so these models may not be inconsistent with experimental results.

Astonishingly enough if $m_D \sim 1 \text{ TeV}$ then gravitons may be readily produced in accelerator experiments. This is because the extra dimensions give an increased phase space for graviton radiation. Another way of looking at this situation is to interpret gravitons which move parallel to the 4 dimensions of space time as the usual gravitons giving rise to Newtonian gravity while the gravitons with momentum components perpendicular to the brane are effectively a continuum of massive objects. The density of gravitons states is given by [2, 3, 5, 6]:

$$D(m^2) = \frac{dN}{dm^2} = \frac{1}{2} S_{n-1} \frac{\bar{M}_P^2 m^{n-2}}{m_D^{n+2}} , \quad (2)$$

where m is the mass of the graviton, $\bar{M}_P = M_P/\sqrt{8\pi}$ and $S_k = 2\pi^{(k+1)/2}/\Gamma[(k+1)/2]$. The probability of graviton emission may thus become large when the sum over the huge number of graviton modes is considered. Of course this distribution cannot increase in

this way forever. At energies $> m_D$ the effects of the fundamental theory should become manifest and so we will suppose that the distribution is cutoff at $\sim m_D$.

Gravitons with polarizations that lie entirely within the physical dimensions are effective spin 2 objects. Gravitons with polarizations partially or completely perpendicular to the physical brane are vector and scalar objects. Processes that are sensitive to the scalar states are of particular interest because the scalar couplings are proportional to mass and so are often weakly coupled to processes exclusively involving particles of low mass.

The prospect that a realistic compactification of M-theory leads to processes that can be readily observed has lead to considerable phenomenological activity [5]-[12]. Broadly speaking there are two kinds of processes where the effects due to this form of gravitation may be detected. First of all, a real graviton may be produced which leaves the detector resulting in a signature involving missing mass and energy, see e.g., [8, 9]. One advantage of this class of reactions is that if a signal is seen, the missing mass spectrum would give strong evidence that these gravity theories are involved and indicate the value of n . The disadvantage is that the rates tend to be suppressed at large n due to the lower density of states; hence the limits that may be set on m_D tend to be less restrictive at larger n .

Secondly, there are processes mediated by virtual gravitons, see e.g., [10, 11, 12]. When a virtual graviton is exchanged, each of the graviton states adds to the amplitude coherently, thus in the sum over gravitons the density of states cancels the $1/M_P^2$ from the gravitational coupling. The disadvantage of these processes is that if a signal is seen, it is unlikely to be easy to prove that gravitational interaction is responsible as opposed to some other new physics. Of course if a limit is being set by the absence of a signal, this is not a problem. The advantage of these processes is that the whole tower of graviton states acts coherently so the results are largely independent of n . Limits can thus be set on all values of n simultaneously. In this paper we will consider process which are of the latter type.

In any virtual process, there will in general exist some Standard Model (SM) background. Clearly it is beneficial to choose processes where the SM background is so small that it does not limit the bound that can be placed on m_D . The class of process which we consider here are of the form $V_1 V_2 \rightarrow V_3 V_4$ where V_i are SM gauge bosons which may be distinct or identical. If the tree level coupling between these four specific bosons does not follow from the gauge theory, then the scattering proceeds only at fourth order in the gauge coupling and is therefore highly suppressed as is the case e.g. for $\gamma\gamma \rightarrow \gamma\gamma$, $ZZ \rightarrow ZZ$ or $gg \rightarrow \gamma\gamma$, $gg \rightarrow ZZ$.

For each of the virtual processes of the form $V_1 V_2 \rightarrow V_3 V_4$ which involve the exchange of gravitons, we need to sum the propagator over all of the possible graviton states. The amplitudes considered here can be factored into one of the following forms:

- (a) $\mathcal{M} = (i/(s - m^2)) \kappa^2 \hat{\mathcal{M}}_s$,
- (b) $\mathcal{M} = (i/(t - m^2)) \kappa^2 \hat{\mathcal{M}}_t$,
- (c) $\mathcal{M} = (i/(u - m^2)) \kappa^2 \hat{\mathcal{M}}_u$,

where m is the mass of the graviton and all the m dependence is in the propagator factor. Also, $\kappa = \sqrt{16\pi G_N}$ [6], where G_N is the Newtonian gravitational constant.

In case (a), for example, the total amplitude including all graviton exchanges is thus:

$$\mathcal{M}_s^{tot} = \hat{\mathcal{M}}_s \sum_{\nu} \frac{i}{s - m_{\nu}^2}, \quad (3)$$

where ν indexes the graviton masses m_{ν} . We write the sum:

$$\sum_{\nu} \frac{i}{s - m_{\nu}^2} = D(s), \quad (4)$$

where the value of $D(s)$ calculated in [5, 6] is:

$$\kappa^2 D(s) = -i \frac{16\pi}{m_D^4} F + O\left(\frac{s}{m_D^2}\right). \quad (5)$$

The constant F contains all the dependence on n and is given by:

$$F = \begin{cases} \log(s/m_D^2) & \text{for } n = 2 \\ 2/(n - 2) & \text{for } n > 2 \end{cases}. \quad (6)$$

Likewise for the t -channel, we can define:

$$\sum_{\nu} \frac{i}{t - m_{\nu}^2} = D_E(t), \quad (7)$$

and similarly for the u -channel. In the case of a $2 \rightarrow 2$ process, to lowest order in s/m_D^2 , $D_E(t) = D_E(u) = D(s)$ [6]. Thus, in general, the sum of all three channels is:

$$\mathcal{M} \approx \kappa^2 D(s) (\hat{\mathcal{M}}_s + \hat{\mathcal{M}}_t + \hat{\mathcal{M}}_u) \approx -i \frac{16\pi}{m_D^4} F (\hat{\mathcal{M}}_s + \hat{\mathcal{M}}_t + \hat{\mathcal{M}}_u). \quad (8)$$

Defining $z = \cos \theta$ where θ is the angle between V_1 and V_3 in the cms frame, the differential cross section is thus given by:

$$\frac{d\sigma}{dz} = \left(\frac{8\pi F^2}{sm_D^8 B \mathcal{P}} \right) \left(\frac{2|\vec{P}_3|}{\sqrt{s}} \right) \sum_{polarization, color} \left| \hat{\mathcal{M}}_s + \hat{\mathcal{M}}_t + \hat{\mathcal{M}}_u \right|^2 \quad (9)$$

where $B = 2$ for identical final state particles and 1 otherwise while \mathcal{P} is the number of initial color times polarization states averaged over.

2 Gauge Boson Scattering

Let us first enumerate some of the instances of this kind of scattering which can be of interest. We will break it down into the following categories:

- Z and γ only:

$$\begin{array}{ll} \text{(a)} & \gamma\gamma \rightarrow \gamma\gamma \\ \text{(b)} & \gamma\gamma \rightarrow ZZ \\ \text{(c)} & ZZ \rightarrow \gamma\gamma \\ \text{(d)} & \gamma Z \rightarrow \gamma Z \end{array} \quad (10)$$

- 2 W 's with Z , W and γ :

$$\begin{array}{ll} \text{(e)} & \gamma\gamma \rightarrow W^+W^-; W^+W^- \rightarrow \gamma\gamma \\ \text{(f)} & W\gamma \rightarrow W\gamma \\ \text{(g)} & ZZ \rightarrow W^+W^-; W^+W^- \rightarrow ZZ \\ \text{(h)} & WZ \rightarrow WZ \\ \text{(i)} & W^+W^- \rightarrow W^+W^-; W^-W^- \rightarrow W^-W^- \end{array} \quad (11)$$

- Processes with 2 gluons

$$\begin{array}{ll} \text{(j)} & gg \rightarrow \gamma\gamma; \gamma\gamma \rightarrow gg \\ \text{(k)} & g\gamma \rightarrow g\gamma \\ \text{(l)} & gg \rightarrow ZZ; ZZ \rightarrow gg \\ \text{(m)} & gZ \rightarrow gZ \\ \text{(n)} & gg \rightarrow WW; WW \rightarrow gg \\ \text{(o)} & gW \rightarrow gW \end{array} \quad (12)$$

- Four gluon coupling:

$$\text{(p)} \quad gg \rightarrow gg \quad (13)$$

- Four Z coupling:

$$\text{(q)} \quad ZZ \rightarrow ZZ \quad (14)$$

These processes will proceed through the Feynman diagrams shown in Fig. 1 where the dashed line represents a spin 2 or spin 0 graviton. The exchange may be in various combinations of the s , t and u -channels depending on what the external bosons are. The spin 0 exchange is only operative if all of the bosons are massive, specifically (g), (i), (h), and (q).

Diagrams which contain either 4 gluons as in case (p), at least 2 W 's as in cases (e)-(h) and 4 Z 's as in case (q) can proceed through tree level SM processes and so the possible large backgrounds must be considered. The other processes will not have tree level SM backgrounds. In what follows we will not consider any process involving W -bosons such as in cases (e)-(h), (n) and (o). We will also not explicitly consider the processes $ZZ \rightarrow gg$ (case (l)) and $gZ \rightarrow gZ$ (case (m)). We note, however, that the formulae we give in the appendices can be easily generalized to include those processes for future use.

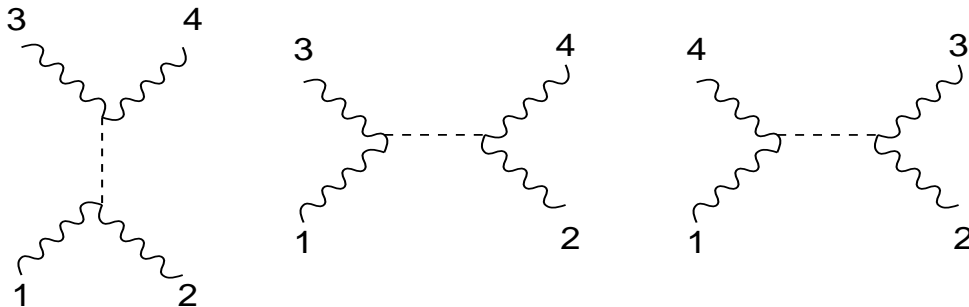


Figure 1: *The three Feynman diagrams that give rise to gauge boson scattering through virtual graviton exchange. Dashed lines stand for the exchanges of a spin 2 or a spin 0 graviton.*

3 Electron-Positron Colliders

To experimentally study the scattering of gauge bosons it is usually necessary to consider reactions where the initial state consists of fermions, in particular e^+ , e^- , p or \bar{p} . At high

energies virtual gauge bosons are then produced nearly on shell and collinear with the initial particles. If one uses the effective boson approximation [13, 14] one may regard the fermion beams as sources of gauge bosons and at leading log ignore the virtuality of these bosons in calculating the cross section.

At electron-positron colliders a number of reactions of this type involving bosons may be studied. The simplest is perhaps $\gamma\gamma \rightarrow \gamma\gamma$. It should be noted, however, that an electron-positron collider can be converted into an almost monochromatic photon-photon collider using back-scatter laser technique [15]. An NLC running in such a photon mode has an advantage that the initial photons may be polarized. In fact, the reaction $\gamma\gamma \rightarrow \gamma\gamma$ has been considered before in [11] in the context of a photon-photon collider. There it was shown that the discovery reach of low energy gravity through the process $\gamma\gamma \rightarrow \gamma\gamma$ may be considerably improved if the initial photons are polarized. The same sensitivity to the initial photons polarization was also found in [12] for the reactions $\gamma\gamma \rightarrow W^+W^-, ZZ$.

Here, we wish instead to explore yet another aspect of this type of $V_1V_2 \rightarrow V_3V_4$ scattering processes, namely, virtual gauge boson emission from the initial e^+e^- of a NLC running in its “simple” mode¹. Clearly, in the case of $V_1 = V_2 = \gamma$, $\gamma\gamma \rightarrow VV$ will then lead to a signature of the form $e^+e^- \rightarrow VVe^+e^-$ which is different from the hard process $\gamma\gamma \rightarrow VV$ (directly observable in a photon-photon collider) and has its own kinematic characteristics.

For instance, in the case of an electron-positron collider, two photon processes are thus calculated using the equivalent photon approximation so that if a cross section $\sigma_{\gamma\gamma \rightarrow X}$ is known, the cross section for $e^+e^- \rightarrow e^+e^- + X$ via the two photon mechanism is given by:

$$\sigma_{e^+e^- \rightarrow e^+e^- X} = \left(\frac{\alpha}{2\pi} \log(s_0/4\hat{m}_e^2) \right)^2 \int_0^1 f(\tau) \sigma_{\gamma\gamma \rightarrow X}(\tau s_0) d\tau, \quad (15)$$

where s_0 is the square of the center of mass energy of the initial e^+e^- and:

$$f(\tau) = \frac{1}{\tau} \left((2+\tau)^2 \log \frac{1}{\tau} - 2(1-\tau)(3+\tau) \right). \quad (16)$$

In this expression the total cross section for $e^+e^- \rightarrow e^+e^- + X$ is given if one takes $\hat{m}_e = m_e$ as the mass of the electron. If one wishes, however to observe the e^+e^- in the final state, experimental considerations suggest that a minimum cut on the transverse

¹For definiteness we discuss gauge boson scattering in an electron-positron collider. Our results below, however, are clearly extendable to muon colliders as well.

momentum of the final state electrons P_{Tmin} be used. In this case the result is given by taking $\hat{m}_e = P_{Tmin}$. For instance, if one is considering the production of real gravitons as in [9], it is essential to observe these final state electrons since the graviton itself is undetectable.

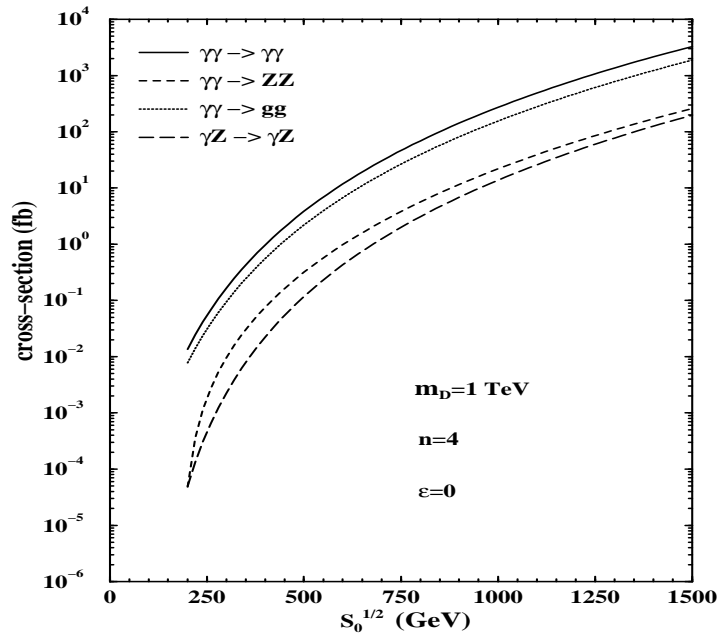


Figure 2: The overall cross sections $\sigma(e^+e^- \rightarrow V_1V_2e^+e^-)$, where $V_i = \gamma, Z$ or g , for various channels of effective gauge boson scattering sub-processes in an electron-positron collider, as a function of the center of mass energy of the collision, $\sqrt{s_0}$. In all the curves we take $m_D = 1$ TeV and $n = 4$. The $\gamma\gamma \rightarrow \gamma\gamma$ sub-process is shown with a solid line, the $\gamma\gamma \rightarrow ZZ$ sub-process is shown with a short dashed line, the $\gamma\gamma \rightarrow gg$ sub-process is shown with a dotted line and the $\gamma Z \rightarrow \gamma Z$ sub-process is shown with a long dashed line.

It is well known [13, 14] that at high energy colliders this expression can be generalized to cases where the photons are replaced with W or Z bosons; in those cases one must generally use helicity dependent structure functions for the initial state gauge bosons.

The helicity amplitudes and cross section for $\gamma\gamma \rightarrow \gamma\gamma$ are given in appendix A (eqs. (A.1)–(A.3)) and the corresponding full cross section, $\sigma(e^+e^- \rightarrow \gamma\gamma e^+e^-)$, is shown in Fig. 2 as a function of $\sqrt{s_0}$ for the case where $n = 4$ (or equivalently $F = 1$, see eq. (6)) and $m_D = 1$ TeV.

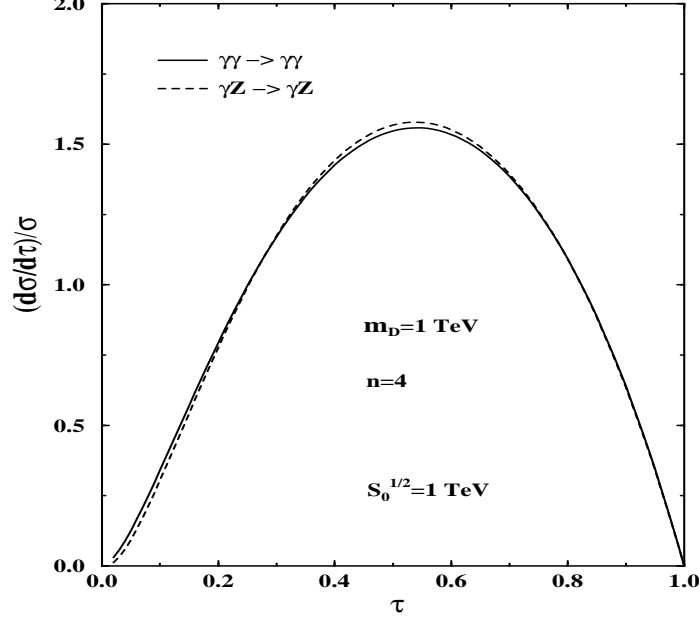


Figure 3: The normalized invariant mass distribution $(d\sigma/d\tau)/\sigma$ is shown for $e^+e^- \rightarrow \gamma\gamma e^+e^-$ via the sub-process $\gamma\gamma \rightarrow \gamma\gamma$ (solid line) and for $e^+e^- \rightarrow \gamma Z e^+e^-$ via the sub-process $\gamma Z \rightarrow \gamma Z$ (dashed line), where $\sqrt{s_0} = 1 \text{ TeV}$. The other model parameters are the same as in Fig. 2.

In Fig. 3 we show the normalized distribution of $(d\sigma/d\tau)/\sigma$, where $\tau = s/s_0$, from which it is clear that most of these events are concentrated at high invariant $\gamma\gamma$ mass. Thus a large portion of the events that make up this cross section would be quite distinctive. This follows from the fact that the cross section is proportional to s^3 ; hence, even though the effective luminosity distribution of the photons decreases at large τ , the growth of the cross section with τ makes the average value of τ become large. The same trend is also true for all of the other reactions considered and so experimental tests for these type of processes should focus on final states of large invariant mass.

Since $\sigma(\gamma\gamma \rightarrow \gamma\gamma)$ (and therefore $\sigma(e^+e^- \rightarrow \gamma\gamma e^+e^-)$) is proportional to F^2/m_D^8 , the value of the cross section may be trivially adjusted for other values of these input parameters; the same is also true for all the other processes which we consider below. Thus, for instance, if $\sqrt{s_0} = 1 \text{ TeV}$, then the cross section is $\sim 270 \text{ fb}$ with $m_D = 1 \text{ TeV}$, so at such an accelerator with a luminosity of 200 fb^{-1} , the limit which could be placed

on m_D with a criterion of 10 events (i.e., assuming that such a signal is observable only if 10 or more events are seen) would be $m_D \sim 2.9 \text{ TeV}$. This limit is weaker than the one achievable in a photon-photon collider using polarized initial photons by about a factor of two (see [11]), but is independently useful for an electron-positron collider.

The amplitude for $\gamma\gamma \rightarrow gg$ is simply the s -channel of the $\gamma\gamma \rightarrow \gamma\gamma$ graph. The helicity amplitudes and cross section for this process are given in appendix B (eqs. (B.1)–(B.3)). The cross section $\sigma(e^+e^- \rightarrow gge^+e^-)$ is also shown in Fig. 2; it is similar to the $\gamma\gamma$ final state and in principle leads to similar sensitivity to m_D . The events in this case would consist of two jets which would typically have a high invariant mass as with the $\gamma\gamma$ events above.

Another class of reactions which may be of interest at electron-positron colliders is reactions which contain Z -bosons in the initial and/or final states. For instance $\gamma\gamma \rightarrow ZZ$ which has been studied in [12] in the context of a photon-photon collider. We note again that the NLC in its photon mode and with polarized initial photons can place stringer limits on m_D [12] by studying $\gamma\gamma \rightarrow ZZ$. Nonetheless, as shown below, it is clearly important to analyze this process in an electron-positron collider as well. The helicity amplitudes and cross section for this process are given in appendix D (eqs. (D.1)–(D.3)) and the cross section is plotted in Fig. 2. This process is smaller than $\gamma\gamma \rightarrow \gamma\gamma$ since it only proceeds through one channel and also smaller than the similar $\gamma\gamma \rightarrow gg$ by roughly the color factor of 8. It does, however, have the prospect of providing information about the polarization of the Z 's from analysis of their decay distributions. In the limit of large $s \gg m_Z^2$, the ratio of longitudinal Z -pairs in comparison to transverse pairs approaches $1/12$ if indeed gravitational interactions are responsible for $\gamma\gamma \rightarrow ZZ$. In particular:

$$\left(\frac{Z_L Z_L}{Z_T Z_T} \right)_{\text{graviton}} = \frac{1}{12} (1 + 4x_Z)^2, \quad (17)$$

where $x_Z = m_Z^2/s$. This may be useful in distinguishing Z pairs produced by gravitons from those produced by other new physics mechanisms. For instance, Higgs or other massive scalar can be produced in the s -channel via $\gamma\gamma$ fusion and decay to a ZZ pair. This would produce a predominance of longitudinally polarized Z 's given by [16]:²

²As discussed below, there is, however, a tree level SM background to the ZZe^+e^- final state coming from exchanges of the SM Higgs boson in the $ZZ \rightarrow ZZ$ sub-process. Such Higgs exchanges in the t and u -channel will have a different (from the one given in eq. (17)) ratio of $Z_L Z_L/Z_T Z_T$. However, since the ZZ luminosity functions are much smaller than the $\gamma\gamma$ ones, we expect the ratio $Z_L Z_L/Z_T Z_T$ to be dominated by the gravity mediated $\gamma\gamma \rightarrow ZZ$ sub-process if indeed the gravity scale is at the 1 TeV level. Moreover, as further mentioned below, the processes $\gamma\gamma \rightarrow ZZ$ and $ZZ \rightarrow ZZ$ may be distinguished by studying the final state electrons.

$$\left(\frac{Z_L Z_L}{Z_T Z_T}\right)_{\text{scalar}} = \frac{(2 - x_Z)^2}{2x_Z^2}. \quad (18)$$

One could also consider the reverse process $ZZ \rightarrow \gamma\gamma$; however, this would probably not be of experimental interest since the smaller ZZ luminosity function would cause it to be about 100 times smaller than the $\gamma\gamma \rightarrow \gamma\gamma$ process with the same final state. The crossed graph $\gamma Z \rightarrow \gamma Z$, however, could have a significant cross section similar to the case of $\gamma\gamma \rightarrow ZZ$.³ In this case the electron which emits the Z would typically have transverse momentum $P_T \sim m_Z$ and hence would be easily detectable providing additional constraints on the kinematics of the final state.

Since both $\gamma\gamma \rightarrow ZZ$ and $\gamma Z \rightarrow \gamma Z$ are about 10 times smaller than $\gamma\gamma \rightarrow \gamma\gamma$ these modes would not be primarily useful in putting a bound on m_D . However, if a graviton signal were seen in the $\gamma\gamma \rightarrow \gamma\gamma$ channel, the ratio $\gamma\gamma : \gamma Z : ZZ$ would be useful in indicating that gravitational interactions were indeed the explanation since this ratio would be independent of m_D and n in the propagator summation approximation discussed above.

The process $ZZ \rightarrow ZZ$ potentially has the unique feature that the exchanged graviton can be either scalar or tensor. We find, however, that numerically the cross section in the context of an e^+e^- collider is not greatly sensitive to the scalar sector. This is partly because there is a similar contribution to the scalar exchanges in Fig. 1 coming from the SM Higgs boson. The helicity amplitudes for the process $ZZ \rightarrow ZZ$, for both the graviton and the SM Higgs exchanges are given in appendix G.

In fact, even assuming for simplicity an infinitely heavy Higgs, i.e., disregarding the SM background to this process, the scalar graviton contribution is rather small as compared to the spin 2 graviton. In particular, in order to test the sensitivity to the scalar sector in $ZZ \rightarrow ZZ$ in the absence of the SM diagrams, we can multiply the scalar propagator by $(1 + \epsilon)$, where ϵ is an arbitrary constant. Using this, the helicity amplitudes for this process, due to the spin 0 (and the spin 2) graviton exchanges are given in appendix G. Note that the only term proportional to R (hence sensitive to the scalar graviton), which is not suppressed at large s by a factor of $x_Z = m_Z^2/s$, is that corresponding to the 0000 helicity combination. This is because the coupling of the scalar graviton to a ZZ pair is

³We note that, for massive vector bosons, the effective vector boson approximation in leading log tends to over estimate the cross section, in particular, the cross section coming from fusion of transversely polarized gauge bosons, see e.g., Johnson *et al.* in [13]. Therefore, the actual overall cross section from $\gamma Z \rightarrow \gamma Z$ may be slightly smaller than what is shown in Fig. 2. For the point we are making, however, the leading log approximation suffices.

explicitly proportional to the mass-squared of the Z [6]. However, when this is coupled to a longitudinal state, this dependence is canceled by the explicit $1/m_Z$ mass dependence due to each of the four longitudinal polarization vectors.

To get an idea of the sensitivity of the graviton cross section to ϵ let us define:

$$r(\epsilon) = \frac{\sigma(\epsilon)}{\sigma(\epsilon = 0)} - 1 . \quad (19)$$

Thus, if $n = 4$, then for $s_0 = 1 \text{ TeV}$, $r(1) = 0.009$, $r(5) = 0.064$, and $r(10) = 0.18$. On the other hand, if $\sqrt{s_0} = 500 \text{ GeV}$, then $r(1) = 0.05$, $r(5) = 0.31$ and $r(10) = 0.80$. Therefore, probably a non-zero value of ϵ leads to unobservably small effects unless ϵ is fairly large, $\epsilon \gg 1$. The reason for this is that the contribution from the scalar exchange is dominated by the case where the initial bosons are longitudinal but the kernel for $e \rightarrow eZ_L$ does not receive logarithmic enhancement as in the case for transverse Z emission. The scalar graviton contribution to the final cross section in the overall reaction is thus modest even though the hard cross section for $Z_L Z_L \rightarrow Z_L Z_L$ via scalar exchange is comparable to the hard cross section for $Z_T Z_T \rightarrow Z_T Z_T$ via tensor exchange. Likewise, if one measures the proportion of longitudinal and transverse Z bosons in the final state, the sensitivity to the scalar exchanged may be increased, however, in reality the SM Higgs contribution will probably dominate the scalar dynamics in this process.

The final state in the case of $ZZ \rightarrow ZZ$ is the same as that of $\gamma\gamma \rightarrow ZZ$; however, the two processes may be separated by observation of the final state electrons. For instance, if we impose the cut that $P_T > m_Z$ for each of the final state electrons at $\sqrt{s_0} = 1 \text{ TeV}$, the $\gamma\gamma \rightarrow ZZ$ is reduced by a factor of about 70 while the signal due to $ZZ \rightarrow ZZ$ is reduced by a factor of about 1.3. Using this cut then, the contribution of $ZZ \rightarrow ZZ$ may thus be enhanced relative to $\gamma\gamma \rightarrow ZZ$.

4 Hadronic Colliders

At hadronic colliders such as the LHC, gauge boson pairs may be produced via graviton exchange in gluon gluon collisions. In particular, let us first consider $gg \rightarrow \gamma\gamma$ and $gg \rightarrow ZZ$. The parton cross section for $gg \rightarrow \gamma\gamma$ is the same as $\gamma\gamma \rightarrow gg$ reduced by a factor of 64 because of color averaging (see appendix B). Likewise, the parton cross section for $gg \rightarrow ZZ$ is the same as $\gamma\gamma \rightarrow ZZ$ reduced by 8 to take into account color (see appendix D). The differential cross section as a function of τ is shown in Fig. 4 in the case of $\gamma\gamma$ production and in Fig. 5 in the case of ZZ production, where a cut of $|z| < 0.7$ has been applied.

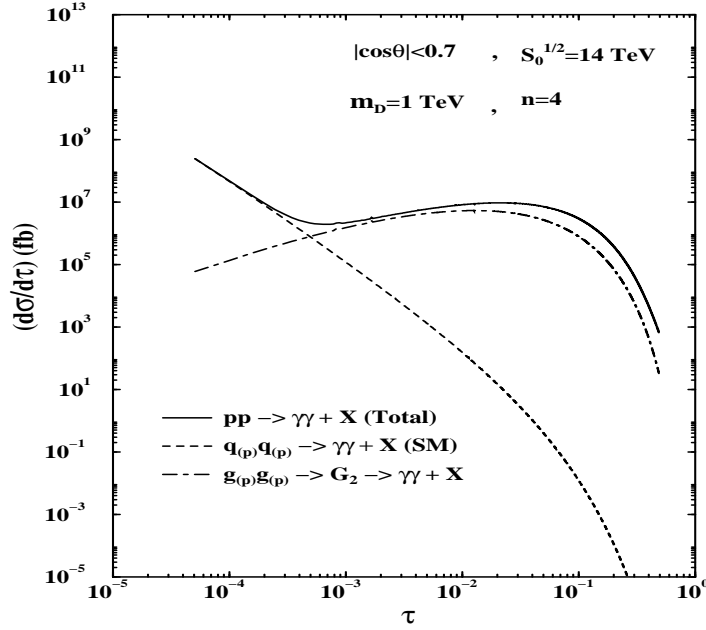


Figure 4: The distribution of $pp \rightarrow \gamma\gamma + X$ events as a function of τ at the LHC for various sub-processes, where in each case a cut of $|\cos\theta| < 0.7$ is imposed. Shown are the total (solid line) $pp \rightarrow \gamma\gamma + X$ cross section from gg and $q\bar{q}$ fusion processes including the graviton exchange and the SM contributions, only the SM cross section from $q\bar{q} \rightarrow \gamma\gamma$ (dashed line) and only the graviton exchange cross section from $gg \rightarrow \gamma\gamma$ (dot-dashed line). The model parameters are the same as in Fig. 2.

In both cases, there is also a contribution from $q\bar{q} \rightarrow \gamma\gamma, ZZ$ due to s -channel graviton exchange. These $q\bar{q}$ annihilation processes also have a SM contribution. The differential cross sections for $q\bar{q} \rightarrow \gamma\gamma$ and $q\bar{q} \rightarrow ZZ$, including the SM, graviton mediated and SM \times graviton interference terms, are given in appendix H.

We note that the effects of graviton exchanges at the Tevatron via the processes $gg \rightarrow \gamma\gamma$ and $q\bar{q} \rightarrow \gamma\gamma$ were studied in detail by Cheung in [11]. Here we focus instead on the LHC in which case the dominant contribution to $\gamma\gamma + X$ production comes from the gluon fusion sub-process as opposed to the Tevatron where $q\bar{q} \rightarrow \gamma\gamma$ is more important. As will be shown below, the attainable limit on m_D at the LHC from $pp \rightarrow \gamma\gamma + X$ is much stronger than the one obtained by Cheung in [11].

In Figs. 4 and 5 we plot the invariant mass distribution, $d\sigma/d\tau$, for the total cross

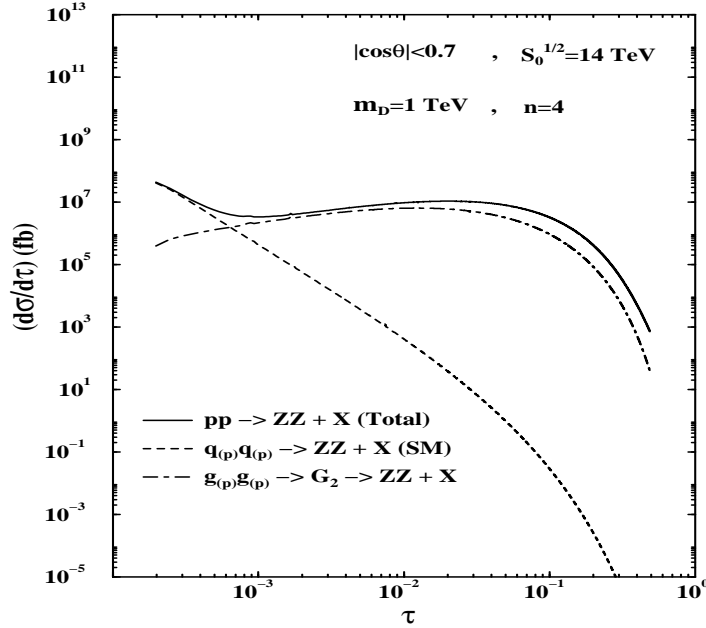


Figure 5: *The distribution of $pp \rightarrow ZZ + X$ events as a function of τ at the LHC for various sub-processes, where in each case a cut of $|\cos\theta| < 0.7$ is imposed. Shown are the total (solid line) $pp \rightarrow ZZ + X$ cross section from gg and $q\bar{q}$ fusion processes including the graviton exchange and the SM contributions, only the SM cross section from $q\bar{q} \rightarrow ZZ$ (dashed line) and only the graviton exchange cross section from $gg \rightarrow ZZ$ (dot-dashed line). The model parameters are the same as in Fig. 2.*

section (i.e., including the SM and graviton contributions from $gg \rightarrow \gamma\gamma, ZZ$ and $q\bar{q} \rightarrow \gamma\gamma, ZZ$), the SM background from $q\bar{q} \rightarrow \gamma\gamma, ZZ$ and the graviton cross section due to the gluon fusion process only. Here and in what follows, the corresponding overall cross sections of the colliding protons are calculated using the CTEQ4M parton distributions [17]. We see that the gluon fusion process is the dominant production mechanism from graviton exchanges. Moreover, as in the case of the electron-positron collider, the cross section peaks at relatively large τ in marked contrast to the SM background which falls off sharply with τ . Clearly, events with such large τ would be a distinctive signature of new physics at the LHC with negligible SM background.

In Fig 7 we show the 3σ limits that can be placed on the scale of the gravitational interactions m_D at the LHC, by measuring $pp \rightarrow \gamma\gamma, ZZ + X$. The limits are obtained

by requiring:

$$\frac{\sigma_{M_{VV}^{min}}^T - \sigma_{M_{VV}^{min}}^{SM}}{\sqrt{\sigma_{M_{VV}^{min}}^T}} \times \sqrt{L} > 3, \quad (20)$$

where $\sigma_{M_{VV}^{min}}^T$ is the total cross section for $\gamma\gamma$ or ZZ production at the LHC integrated from a lower VV invariant mass cut of M_{VV}^{min} ($V = \gamma$ or Z), and $\sigma_{M_{VV}^{min}}^{SM}$ is the corresponding SM cross section for these processes. Also, we take an integrated luminosity of $L = 30 \text{ fb}^{-1}$ and we require at least 10 such events above the SM background for the given value of m_D^{min} - the lower bound on m_D (see [18]).

As stated before, since the SM cross sections for these type of processes drop sharply with M_{VV} , it is advantageous to study these cross sections at high M_{VV} in which case one is eliminating a large portion of the SM background. Clearly, as can be seen in Fig. 7, there is an optimal lower cut, M_{VV}^{min} , that one can impose on these signals in order to place the best limits on m_D in case no deviation from the SM is observed. This is because as one further goes to higher M_{VV} values, the gravitational signal sharply falls as well. For example, for $\gamma\gamma$ and ZZ production, the optimal lower cuts to be considered are $M_{\gamma\gamma}^{min} \sim M_{ZZ}^{min} \approx 2 \text{ TeV}$, in which case the obtainable bound at the LHC (with $L = 30 \text{ fb}^{-1}$) will be $m_D \gtrsim 6 \text{ TeV}$. We note that, for $m_D = 6 \text{ TeV}$ and $M_{\gamma\gamma}^{min} = 2 \text{ TeV}$, $\sigma_{M_{\gamma\gamma}^{min}}^T(pp \rightarrow \gamma\gamma + X) \simeq 0.7 \text{ fb}$ and $\sigma_{M_{\gamma\gamma}^{min}}^{SM}(pp \rightarrow \gamma\gamma + X) \simeq 0.1 \text{ fb}$, yielding about ~ 20 $\gamma\gamma$ events out of which ~ 17 are due to gravitational interactions. Also, this limit is more than four times larger than the one found by Cheung in [11] for the upgraded Tevatron run II case. The corresponding cross sections for ZZ production with $m_D = 6 \text{ TeV}$ and $M_{ZZ}^{min} = 2 \text{ TeV}$ are: $\sigma_{M_{ZZ}^{min}}^T(pp \rightarrow ZZ + X) \simeq 0.9 \text{ fb}$ and $\sigma_{M_{ZZ}^{min}}^{SM}(pp \rightarrow ZZ + X) \simeq 0.25 \text{ fb}$, yielding about ~ 30 ZZ events out of which ~ 20 are due to gravitational interactions.

The process $gg \rightarrow W^+W^-$ would be about twice as large as the $gg \rightarrow ZZ$ due to the Bose symmetry factor in the latter. The final state however would be more difficult to observe experimentally.

Another process which may be studied at hadronic colliders is pp or $p\bar{p} \rightarrow 2 \text{ jets} + X$. At the LHC, $gg \rightarrow gg$ and $gg \rightarrow q\bar{q}$ will be the dominant production mechanism of 2 jets due to the large gluon content in the colliding protons. These processes can proceed via graviton exchanges where, again, the dominant graviton signal comes from the gluon – gluon scattering sub-process $gg \rightarrow gg$. There will of course be a large 2 jets QCD background from the SM. The SM and gravity mediated amplitudes and cross sections for $gg \rightarrow gg$ and $gg \rightarrow q\bar{q}$ are given in appendix A and H, respectively.

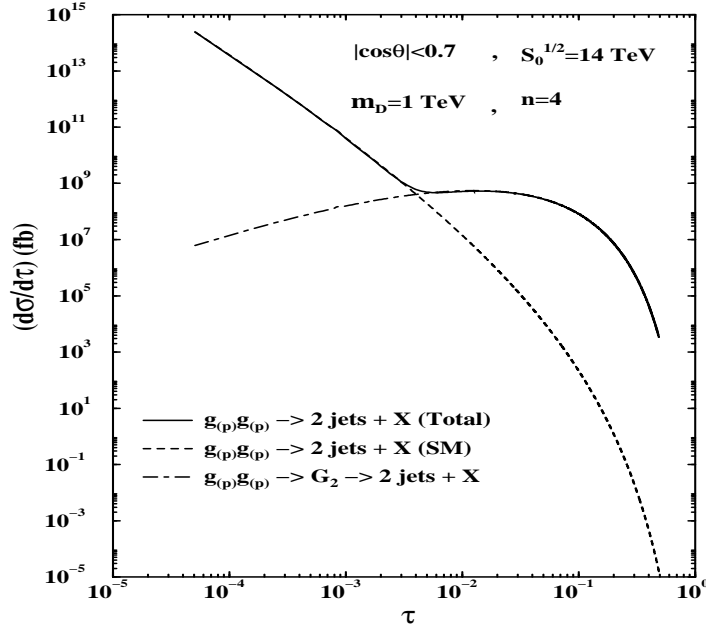


Figure 6: The 2 jets invariant mass distribution of $pp \rightarrow 2 \text{ jets} + X$ events as a function of τ at the LHC for various sub-processes where in each case a cut of $|\cos\theta| < 0.7$ is imposed. Shown are the total (solid line) $pp \rightarrow 2 \text{ jets} + X$ cross section from the gg fusion processes $gg \rightarrow gg, q\bar{q}$ including the graviton exchange and the SM contributions, only the SM cross section from $gg \rightarrow gg, q\bar{q}$ (dashed line) and only the graviton exchange cross section from four gluons scattering sub-process $gg \rightarrow gg$ (dot-dashed line). The model parameters are the same as in Fig. 2.

In Fig. 6 we plot the invariant mass distribution, $d\sigma/d\tau$, of the total cross section for $pp \rightarrow 2 \text{ jets} + X$, of the SM QCD background and of the graviton cross section due only to the pure four gluon scattering process. Evidently, the QCD background is again peaked at low τ while the 2 jet events resulting from graviton exchange occur at large τ .

In Fig 7 we also show the 3σ limits (obtained from eq.(20)) that can be placed on m_D at the LHC, by measuring the dijets events $pp \rightarrow 2 \text{ jets} + X$. For reasons mentioned above, there is again an optimal value of M_{jj}^{min} (M_{jj} is the invariant mass of the 2 jets system) which gives the best limit on m_D . In particular, in this case, cutting the cross section from below by $M_{jj}^{min} \sim 5 \text{ TeV}$, will result in the 3σ limit $m_D \gtrsim 6 \text{ TeV}$, if no deviation from the SM cross section is observed. Again we note that for $m_D = 6 \text{ TeV}$ and

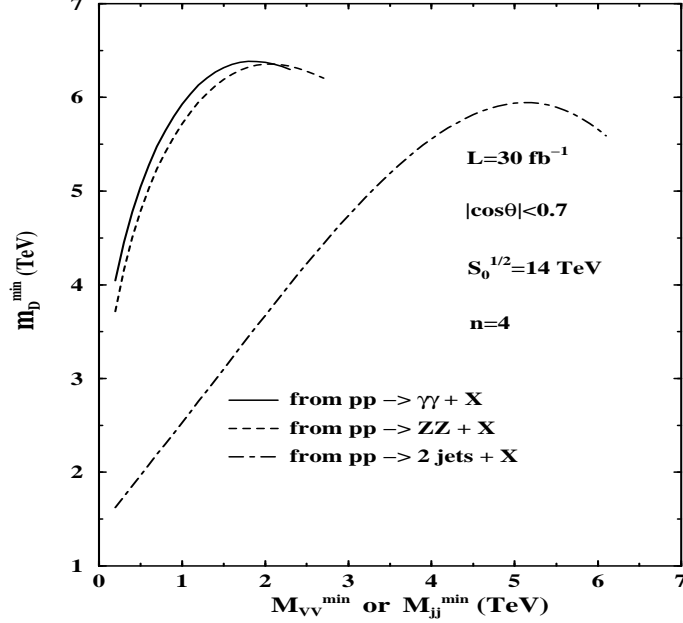


Figure 7: 3σ bounds on the scale m_D of the gravitational interactions derived from eq. (20), as a function of the lower cut on the invariant mass M_{VV}^{\min} or M_{jj}^{\min} of the VV or jj system ($V = \gamma$ or Z and $j=\text{jet}$), see text. Shown are the limits (m_D^{\min}) that can be obtained by using the reactions $pp \rightarrow \gamma\gamma + X$ (solid line), $pp \rightarrow ZZ + X$ (dashed line) and $pp \rightarrow 2 \text{ jets} + X$ (dot-dashed line), where in each case a cut of $|\cos\theta| < 0.7$ is imposed. The bounds are given for a LHC with an integrated luminosity of 30 inverse fb's. The rest of the model parameters are the same as in Fig. 2. See also [18].

$M_{jj}^{\min} = 5 \text{ TeV}$, $\sigma_{M_{jj}^{\min}}^T(pp \rightarrow 2 \text{ jets} + X) \simeq 1.5 \text{ fb}$ and $\sigma_{M_{jj}^{\min}}^{SM}(pp \rightarrow 2 \text{ jets} + X) \simeq 0.8 \text{ fb}$, yielding about ~ 45 jj events out of which ~ 20 are due to gravitational interactions.

5 Summary and conclusion

We have studied gauge boson - gauge boson scattering processes of the form $V_1 V_2 \rightarrow V_3 V_4$, where V_i are SM gauge bosons, due to graviton exchanges. We have shown that these type of processes can lead to some very distinct signatures of gravitational interactions at future colliders, which have no SM background at lowest order in the relevant gauge

couplings.

For example, at an high energy electron-positron collider, vector bosons which are produced nearly on-shell and collinear with the initial particles, can collide and exchange spin 2 and/or spin 0 gravitons, leading to appreciably large new signals such as $\gamma\gamma \rightarrow \gamma\gamma$, gg , ZZ , $\gamma Z \rightarrow \gamma Z$, $ZZ \rightarrow ZZ$ etc... The latter is of particular interest since it has some sensitivity to scalar graviton excitations if, for some reason, these turn out to be enhanced.

Similarly, gauge boson scattering, due to graviton exchanges, which involve two or four gluons, such as $gg \rightarrow \gamma\gamma$, ZZ , WW , gg , can lead to significantly enhanced signals of $\gamma\gamma$, ZZ , WW and jj ($j=\text{jet}$) pair production at the LHC.

A key feature of all these type of scattering processes is that the gravity mediated cross-sections peak at high values of the invariant VV mass, whereas their corresponding SM cross sections (which in some instances arise only at higher orders in the gauge couplings) are concentrated at low τ values. Thus, these type of low energy gravity signals will be quite distinctive.

Alternatively, if no such new signals are observed, then some of these processes can be used to place a bound on the scale of gravitational interactions. For example, we find that a limit of $m_D \gtrsim 3$ TeV can be placed on the scale of the low energy gravity using the reaction $e^+e^- \rightarrow \gamma\gamma e^+e^-$ which proceed predominantly through graviton exchanges in the $\gamma\gamma \rightarrow \gamma\gamma$ sub-process at the e^+e^- Next Linear Collider.

In those cases which have a significant SM background, we utilized the growth of the gravitational cross-sections with τ to derive the best (optimal) limits. For example, we found that $m_D \gtrsim 6$ TeV will be obtainable at the LHC by measuring the production rates of $pp \rightarrow \gamma\gamma$, ZZ , $WW + X$ and $pp \rightarrow 2 \text{ jets} + X$ which, at high τ , are driven predominantly by graviton exchanges in the $gg \rightarrow \gamma\gamma$, ZZ , WW , gg sub-processes.

S.B. thanks Jose Wudka for discussions. This research was supported in part by US DOE Contract Nos. DE-FG02-94ER40817 (ISU), DE-FG03-94ER40837 (UCR) and DE-AC02-98CH10886 (BNL).

Appendices: Helicity amplitudes and cross sections

For each of the processes we discuss, we give the helicity amplitudes, the differential cross section and the cross section. In all cases the scattering is of the general form $V_1 V_2 \rightarrow V_3 V_4$ where V_i is a vector boson with momentum p_i and helicity h_i . The angle between \vec{p}_1 and \vec{p}_3 in the cms frame is θ and $z = \cos \theta$. We also define the quantity $s = (p_1 + p_2)^2$.

A: $\gamma\gamma \rightarrow \gamma\gamma$ and $gg \rightarrow gg$

The helicity amplitudes for these processes, in which the graviton exchange is in all three s , t and u -channels, are:

$$\mathcal{M}_{4\gamma}(h1, h2, h3, h4) = \frac{1}{4}\kappa^2 D \times \begin{cases} 2Q_s s^2 & \text{if } h1 = h2 = h3 = h4 \\ Q_u(1+z)^2 s^2/2 & \text{if } h1 = -h2 = -h3 = h4 \\ Q_t(1-z)^2 s^2/2 & \text{if } h1 = -h2 = h3 = -h4 \\ 0 & \text{otherwise} \end{cases}, \quad (\text{A.1})$$

where for $\gamma\gamma \rightarrow \gamma\gamma$, $Q_s = Q_t = Q_u = 1$ while for $gg \rightarrow gg$, $Q_s = (\delta_{AC}\delta_{BD} + \delta_{AD}\delta_{BC})/2$, $Q_t = (\delta_{AB}\delta_{CD} + \delta_{AD}\delta_{BC})/2$ and $Q_u = (\delta_{AC}\delta_{BD} + \delta_{AB}\delta_{CD})/2$, where A , B , C and D are the color indices for g_1 , g_2 , g_3 and g_4 respectively.

This leads to the following differential and total cross sections, previously derived in [11]:

$$\frac{d\sigma_{2\gamma \rightarrow 2\gamma}}{dz} = \frac{\pi F^2 Q_{tot}}{16s} \left(\frac{s^4}{m_D^8} \right) (z^2 + 3)^2, \quad (\text{A.2})$$

$$\sigma_{2\gamma \rightarrow 2\gamma} = \frac{\pi F^2 Q_{tot}}{s} \left(\frac{s^4}{m_D^8} \right) \left(\frac{7}{5} \right), \quad (\text{A.3})$$

where $Q_{tot} = 1$ for $\gamma\gamma \rightarrow \gamma\gamma$ and $Q_{tot} = 9/16$ for $gg \rightarrow gg$.

In the case of $gg \rightarrow gg$ there is also a SM contribution which is given for example in [14]. The graviton amplitude, therefore, interferes with the tree level SM diagrams. Denoting the interference term by $\sigma_{gg \rightarrow gg}^I$, this interference is given by:

$$\frac{d\sigma_{gg \rightarrow gg}^I}{dz} = -\frac{5}{2} \sqrt{\frac{\pi\alpha_s^2}{s} \left(\frac{d\sigma_{gg \rightarrow gg}}{dz} \right)} , \quad \sigma_{gg \rightarrow gg}^I = -\frac{25}{42} \sqrt{35 \frac{\pi\alpha_s^2}{s} \sigma_{gg \rightarrow gg}} , \quad (\text{A.4})$$

where $\alpha_s = g_s^2/4\pi$ and g_s is the QCD coupling.

B: $\gamma\gamma \rightarrow gg$

In the case of $\gamma\gamma \rightarrow gg$ the graviton exchange is only in the s -channel and the helicity amplitudes are:

$$\mathcal{M}_{2\gamma \rightarrow 2g}(h1, h2, h3, h4) = \frac{1}{16} \kappa^2 D \times \begin{cases} (1+z)^2 s^2 \delta_{AB} & \text{if } h1 = -h2 = h4 = -h3 \\ (1-z)^2 s^2 \delta_{AB} & \text{if } h1 = -h2 = h3 = -h4 \\ 0 & \text{otherwise} \end{cases} , \quad (\text{B.1})$$

where A and B are color indices.

This leads to the differential and total cross sections:

$$\frac{d\sigma_{2\gamma \rightarrow 2g}}{dz} = \frac{\pi F^2}{8s} \left(\frac{s^4}{m_D^8} \right) (z^4 + 6z^2 + 1) , \quad (\text{B.2})$$

$$\sigma_{2\gamma \rightarrow 2g} = \frac{4}{5} \frac{\pi F^2}{s} \left(\frac{s^4}{m_D^8} \right) . \quad (\text{B.3})$$

The cross sections in the reverse reaction $gg \rightarrow \gamma\gamma$ are smaller by a factor of 64 due to color averaging and was also derived by Cheung in [11] with whom we agree.

C: $g\gamma \rightarrow g\gamma$

In this case, the graviton exchange is only in the t -channel and the helicity amplitudes are:

$$\mathcal{M}_{g\gamma \rightarrow g\gamma}(h1, h2, h3, h4) = \frac{1}{4} \kappa^2 D \times \begin{cases} s^2 & \text{if } h1 = h2 = h3 = h4 \\ (1+z)^2 s^2/4 & \text{if } h1 = -h2 = h3 = -h4 \\ 0 & \text{otherwise} \end{cases} , \quad (\text{C.1})$$

which gives a differential and total cross section of:

$$\frac{d\sigma_{g\gamma \rightarrow g\gamma}}{dz} = \frac{\pi F^2}{64s} \left(\frac{s^4}{m_D^8} \right) (17 + 4z + 6z^2 + 4z^3 + z^4) , \quad (\text{C.2})$$

$$\sigma_{g\gamma \rightarrow g\gamma} = \frac{\pi F^2}{s} \left(\frac{s^4}{m_D^8} \right) \left(\frac{3}{5} \right) . \quad (\text{C.3})$$

D: $\gamma\gamma \rightarrow ZZ$ and $gg \rightarrow ZZ$

In the case of $\gamma\gamma \rightarrow ZZ$ the graviton exchange is also only in the s -channel and the helicity amplitudes are given by:

$$\mathcal{M}_{2\gamma \rightarrow 2Z}(h1, h2, h3, h4) = \frac{1}{4} \kappa^2 D s^2 \alpha_{h1, h2, h3, h4}(z, x_Z) , \quad (\text{D.1})$$

where $x_Z = m_Z^2/s$ and we have defined the “reduced” helicity amplitude $\alpha_{h1, h2, h3, h4}$ which is given in Table 1. Note that the amplitude is only non-zero if $h1 = -h2$ so only $\alpha_{+1, -1, h3, h4}$ is given. The case where $h1 = -1$ is clearly related by Parity.

$h1 \ h2 \ h3 \ h4$	$\alpha_{h1, h2, h3, h4}(z, x_Z)$
$+ \ - \ \pm\pm,$	$x_Z(1 - z^2)$
$+ \ - \ \pm 0; + \ - \ 0\mp$	$(x_Z(1 - z^2)/2)^{1/2}(1 \pm z)$
$+ \ - \ \pm\mp$	$(1 \pm z)^2/4$
$+ \ - \ 00$	$-(1 - z^2)(1 + 4x_Z)/4$

Table 1: The reduced helicity amplitude $\alpha_{h1, h2, h3, h4}$, as defined in eq.(D.1), for the process $\gamma\gamma \rightarrow ZZ$ or $gg \rightarrow ZZ$. Values not given are either zero or related to the given values by Parity.

The differential and total cross sections for this process are thus given by:

$$\frac{d\sigma_{2\gamma \rightarrow 2Z}}{dz} = \frac{\pi F^2}{128s} \left(\frac{s^4}{m_D^8} \right) \beta_Z (3 + 4x_Z - 4x_Z z^2 + z^2) (1 + 12x_Z - 12z^2 x_Z + 3z^2) \quad (\text{D.2})$$

$$\sigma_{2\gamma \rightarrow 2Z} = \frac{\pi F^2}{120s} \left(\frac{s^4}{m_D^8} \right) \beta_Z (48x_Z^2 + 56x_Z + 13) , \quad (\text{D.3})$$

where:

$$\beta_Z = \sqrt{1 - 4x_Z} . \quad (\text{D.4})$$

In the case of $gg \rightarrow ZZ$ the cross sections are related to the above by $\sigma_{2g \rightarrow 2Z} = \sigma_{2\gamma \rightarrow 2Z}/8$ due to color.

E: $ZZ \rightarrow \gamma\gamma$

The process $ZZ \rightarrow \gamma\gamma$ is the reverse of $\gamma\gamma \rightarrow ZZ$ so the matrix elements are the same as the reverse process, however in order to analyze the cross section using the effective boson approximation we need to obtain the differential and total cross section for each initial helicity state. These are given by:

$$\frac{d\sigma_{2Z \rightarrow 2\gamma}(h_1, h_2)}{dz} = \frac{\pi F^2}{4s} \left(\frac{s^4}{m_D^8} \right) \beta_Z^{-1} \times \begin{cases} (1 + 6z^2 + z^4)/8 & \text{for } h_1, h_2 = \pm, \mp \\ 2x_Z^2(1 - z^2)^2 & \text{for } h_1, h_2 = \pm, \pm \\ x_Z(1 - z^4) & \text{for } h_1, h_2 = \pm, 0; 0, \pm \\ (1 + 4x_Z)^2(1 - z^2)^2/8 & \text{for } h_1, h_2 = 0, 0 \end{cases} , \quad (\text{E.1})$$

$$\sigma_{2Z \rightarrow 2\gamma}(h_1, h_2) = \frac{\pi F^2}{4s} \left(\frac{s^4}{m_D^8} \right) \beta_Z^{-1} \times \begin{cases} 4/5 & \text{for } h_1, h_2 = \pm, \mp \\ 32x_Z^2/15 & \text{for } h_1, h_2 = \pm, \pm \\ 8x_Z/5 & \text{for } h_1, h_2 = \pm, 0; 0, \pm \\ 2(1 + 4x_Z)^2/15 & \text{for } h_1, h_2 = 0, 0 \end{cases} , \quad (\text{E.2})$$

where β_Z is defined in eq. (D.4) and again $x_Z = m_Z^2/s$.

F: $\gamma Z \rightarrow \gamma Z$

In the case of $\gamma Z \rightarrow \gamma Z$ the reaction proceeds only through the t -channel. The helicity amplitudes for this process are:

$$\mathcal{M}_{\gamma Z \rightarrow \gamma Z}(h1, h2, h3, h4) = \frac{1}{4} \kappa^2 D s^2 \beta_{h1, h2, h3, h4}(z, x_Z) , \quad (\text{F.1})$$

where the reduced helicity amplitudes in this case, $\beta_{h1, h2, h3, h4}$, are given in Table 2.

$h1 \ h2 \ h3 \ h4$	$\beta_{h1, h2, h3, h4}(z, x_Z)$
$++ ++$	$(2 - x_Z + x_Z z)^2 (1 - x_Z)^2 / 4$
$+- ++$	$x_Z (1 - x_Z)^2 (1 - z^2) / 4$
$+- +-$	$(1 - x_Z)^2 (1 + z)^2 / 4$
$++ +0$	$-\sqrt{2} x_Z (1 - z^2) (1 - x_Z)^2 (2 - x_Z + z x_Z) / 4$
$+0 +-$	$-\sqrt{2} x_Z (1 - z^2) (1 - x_Z)^2 (1 + z) / 4$
$+0 +0$	$(1 + z) (1 - x_Z)^2 (1 - x + x_Z z) / 2$

Table 2: *The reduced helicity amplitude $\beta_{h1, h2, h3, h4}$, as defined in eq.(F.1), for the process $\gamma Z \rightarrow \gamma Z$. Values not given are either zero or related to the given values by Parity.*

The total cross section as a function of the initial Z helicity and averaged over the initial photon polarizations is:

$$\sigma_{\gamma Z \rightarrow \gamma Z}(h2) = \frac{\pi F^2}{60s} \left(\frac{s^4}{m_D^8} \right) \times \begin{cases} (1 - x_Z)^4 (36 - 47x_Z + 52x_Z^2 - 27x_Z^3 + 6x_Z^4) & \text{for } h2 = \pm \\ 2(1 - x_Z)^4 (10 + 3x_Z - 6x_Z^2 + 3x_Z^3) & \text{for } h2 = 0 \end{cases} , \quad (\text{F.2})$$

G: $ZZ \rightarrow ZZ$

This process proceeds in all three channels via both spin 2 and spin 0 graviton exchanges and, in the SM, via neutral Higgs exchange. For the graviton exchange the helicity amplitudes for this process are:

$$\mathcal{M}_{2Z \rightarrow 2Z}(h1, h2, h3, h4) = \frac{1}{4} \kappa^2 D s^2 \gamma_{h1, h2, h3, h4}(z, x_Z, R) , \quad (\text{G.1})$$

where the reduced helicity amplitudes $\gamma_{h1, h2, h3, h4}$ are given in Table 3 and $R = 2(1 + \epsilon)(n - 1)/(3n + 6)$ is the factor associated with the scalar propagator as discussed in the text.

$h1 \ h2 \ h3 \ h4$	$\gamma_{h1, h2, h3, h4}^2(z, x_Z)$	$\gamma_{h1, h2, h3, h4}^0(z, x_Z)$
$+-\pm\mp$	$(3 - 6x_Z + 8x_Z^2)(1 \pm z)^2/6$	$2x_Z^2(1 \pm z)^2$
$+-\pm\pm$	$x_Z(9 - 4x_Z)(1 - z^2)/6$	$x_Z^2(1 - z^2)$
$\pm\pm\pm\pm$	$2(24x_Z^2 + 8x_Z^2z^2 - 18x_Z + 3)/3$	$2x_Z^2(z^2 + 3)$
$\pm\pm\mp\mp$	$16x_Z^2z^2/3$	$2x_Z^2(3 + z^2)$
0000	$(3 + 6z^2x_Z - 22x_Z + 24x_Z^2z^2 + 24x_Z^2 + z^2)/3$	$(24x_Z^2 - 16x_Z + 3 + z^2)$
00 $\pm\pm$	$x_Z(15 - 28x_Z - 7z^2 + 36z^2x_Z)/6$	$x_Z(3 - 4x_Z - z^2)$
00 $\pm\mp$	$-(1 - z^2)(3 + 26x_Z - 24x_Z^2)/12$	$-x_Z(1 - z^2)$
000 \pm	$\pm(7 + 36x_Z)z\sqrt{2x_Z(1 - z^2)}/12$	$\pm z\sqrt{2x_Z(1 - z^2)}/2$
0 + 0 \pm ; 0 + \mp 0	$(1 \pm z)(3 - 28x_Z + 32x_Z^2 \pm 16x_Zz)/6$	$-x_Z(1 \pm z)(1 - 2x_Z \mp z)$
0 + $\pm\pm$	$\pm 8z\sqrt{2x_Z^3(1 - z^2)}$	$\pm z\sqrt{2x_Z^3(1 - z^2)}$
0 + $\mp\pm$	$-(1 \pm z)(9 - 4x_Z)\sqrt{2x_Z(1 - z^2)}/12$	$-(1 \pm z)x_Z\sqrt{2x_Z(1 - z^2)}$

Table 3: The reduced helicity amplitude $\gamma_{h1, h2, h3, h4}$, as defined in eq.(G.1), for the process $ZZ \rightarrow ZZ$. We have defined $\gamma_{h1, h2, h3, h4}(z, x_Z, R) = \gamma_{h1, h2, h3, h4}^2(z, x_Z) + R\gamma_{h1, h2, h3, h4}^0(z, x_Z)$, where $R = 2(1 + \epsilon)(n - 1)/(3n + 6)$. See also text. Values not given are related to the given values by Parity.

For the SM Higgs boson exchange the helicity amplitudes for this process are:

$$\mathcal{M}_{2Z \rightarrow 2Z}^{SM}(h1, h2, h3, h4) = \frac{1}{8} g_W^2 \frac{m_Z^2}{m_W^2} s \gamma_{h1, h2, h3, h4}^{SM}(z, x_Z, \Pi_s, \Pi_t, \Pi_u) , \quad (\text{G.2})$$

where $g_W = e/s_W$ is the weak coupling and $\Pi_x = (x - m_H^2 + i\Gamma_H m_H)^{-1}$, $x = s, t, u$, are the s, t and u -channel factors associated with the corresponding SM Higgs propagators, where $t(u) = s(z - (+)1)(4x_Z - 1)/2$. The reduced SM helicity amplitudes $\gamma_{h1, h2, h3, h4}^{SM}$ are given in Table 4.

$h1 \ h2 \ h3 \ h4$	$\gamma_{h1, h2, h3, h4}^{SM}(z, x_Z, \Pi_s, \Pi_t, \Pi_u)$
$+-\pm\mp$	$2x_Z(1 \pm z)^2(\Pi_t + \Pi_u)$
$+-\pm\pm$	$2x_Z(1 - z^2)(\Pi_t + \Pi_u)$
$++\pm\pm$	$2x_Z[4\Pi_s + (1 \pm z)^2\Pi_t + (1 \mp z)^2\Pi_u]$
0000	$2[4\Pi_s(1 - 2x_Z)^2 + \Pi_t(z - 1 + 4x_Z)^2 + \Pi_u(z + 1 - 4x_Z)^2]/x_Z$
00 $\pm\pm$	$[4\Pi_s(1 - 2x_Z) + (1 - z^2)(\Pi_t + \Pi_u)]$
00 $\pm\mp$	$-(1 - z^2)(\Pi_t + \Pi_u)$
000 \pm	$\pm\sqrt{2x_Z(1 - z^2)}[\Pi_t(z - 1 + 4x_Z) + \Pi_u(z + 1 - 4x_Z)]/2x_Z$
0 $+\pm 0$	$-(1 \mp z)[\Pi_t(z \pm 1) + \Pi_u(z + 1 - 4x_Z)]$
0 $+0\pm$	$(1 \pm z)[\Pi_u(z \mp 1) + \Pi_t(z - 1 + 4x_Z)]$
0 $+\pm\pm$	$\sqrt{2x_Z(1 - z^2)}[\Pi_t(z \pm 1) + \Pi_u(z \mp 1)]$
0 $+\mp\pm$	$-\sqrt{2x_Z(1 - z^2)}(z \pm 1)(\Pi_t + \Pi_u)/2$

Table 4: The reduced helicity amplitude $\gamma_{h1, h2, h3, h4}^{SM}$ for the SM Higgs exchange contribution to the process $ZZ \rightarrow ZZ$, as defined in eq.(G.2). Values not given are related to the given values by Parity. $\Pi_{s, t, u}$ are defined in the text above.

H: $q\bar{q} \rightarrow \gamma\gamma$, $q\bar{q} \rightarrow ZZ$ and $gg \rightarrow q\bar{q}$

Though not gauge-gauge scattering processes, we require $q\bar{q} \rightarrow \gamma\gamma$, $q\bar{q} \rightarrow ZZ$ and $gg \rightarrow q\bar{q}$ for the processes $pp \rightarrow \gamma\gamma + X$, $pp \rightarrow ZZ + X$ and $pp \rightarrow 2 \text{ jets}$, respectively. As in the case of $gg \rightarrow gg$, these processes have a SM contribution and, therefore, also an interference term of the graviton exchange with the SM diagrams.⁴

⁴The differential cross section for $q\bar{q} \rightarrow \gamma\gamma$ including the SM and graviton exchanges was also derived by Cheung in [11]

The pure SM differential cross sections for these processes are:

$$\frac{d\sigma_{q\bar{q}\rightarrow\gamma\gamma}^{SM}}{dz} = \frac{e^4 Q_q^4}{48\pi s} \left(\frac{1+z^2}{1-z^2} \right), \quad (\text{H.1})$$

$$\begin{aligned} \frac{d\sigma_{q\bar{q}\rightarrow ZZ}^{SM}}{dz} &= \frac{e^4}{24\pi s} \frac{(g_L^q)^4 + (g_R^q)^4}{s_W^4(1-s_W^2)^2} \beta_Z \times \\ &\quad \frac{2 + \beta_Z^2(3 - \beta_Z^4) - z^2\beta_Z^2(9 - 10\beta_Z^2 + \beta_Z^4) - 4z^4\beta_Z^4}{[(1 + \beta_Z^2)^2 - 4z^2\beta_Z^2]^2}, \end{aligned} \quad (\text{H.2})$$

$$\frac{d\sigma_{gg\rightarrow q\bar{q}}^{SM}}{dz} = \frac{g_s^4}{1536\pi s} \left(\frac{7 + 16z^2 + 9z^4}{1 - z^2} \right). \quad (\text{H.3})$$

where β_Z is defined in eq. (D.4) and $s_W = \sin \theta_W$, where θ_W is the weak mixing angle. Also, g_L^q and g_R^q are left and right handed couplings of a Z -boson to quarks; for $q = u$ (up quark) $g_L^u = 1/2 - 2s_W^2/3$, $g_R^u = -2s_W^2/3$ and for $q = d$ (down quark) $g_L^d = -1/2 + s_W^2/3$, $g_R^d = -s_W^2/3$.

The pure gravity mediated differential cross sections for these processes are:

$$\frac{d\sigma_{q\bar{q}\rightarrow\gamma\gamma}^G}{dz} = \frac{\pi F^2}{192s} \left(\frac{s^4}{m_D^8} \right) (1 - z^4), \quad (\text{H.4})$$

$$\begin{aligned} \frac{d\sigma_{q\bar{q}\rightarrow ZZ}^G}{dz} &= \frac{\pi F^2}{384s} \left(\frac{s^4}{m_D^8} \right) \beta_Z \times \\ &\quad [4 + 3\beta_Z^4 z^2(1 - z^2) - 2\beta_Z^2(1 + z^2)], \end{aligned} \quad (\text{H.5})$$

$$\frac{d\sigma_{gg\rightarrow q\bar{q}}^G}{dz} = \frac{9}{4} \frac{d\sigma_{q\bar{q}\rightarrow\gamma\gamma}^G}{dz}, \quad (\text{H.6})$$

and the corresponding interference terms are:

$$\frac{d\sigma_{q\bar{q}\rightarrow\gamma\gamma}^I}{dz} = \frac{e^2 Q_q^2 F}{48s} \left(\frac{s^2}{m_D^4} \right) (1 + z^2), \quad (\text{H.7})$$

$$\begin{aligned} \frac{d\sigma_{q\bar{q}\rightarrow ZZ}^I}{dz} &= \frac{e^2 F}{48s} \frac{(g_L^q)^2 + (g_R^q)^2}{s_W^2(1-s_W^2)} \beta_Z \times \\ &\quad \frac{-2 - \beta_Z^2(1 - \beta_Z^2) + 5z^2\beta_Z^2(1 - \beta_Z^2) + 2z^4\beta_Z^4}{(1 + \beta_Z^2)^2 - 4z^2\beta_Z^2}, \end{aligned} \quad (\text{H.8})$$

$$\frac{d\sigma_{gg\rightarrow q\bar{q}}^I}{dz} = \frac{3}{8} \frac{d\sigma_{q\bar{q}\rightarrow\gamma\gamma}^I}{dz}. \quad (\text{H.9})$$

References

- [1] P. Ginsparg, Phys. Lett. **B197**, 139 (1987); I. Antoniadis, Phys. Lett. **B246**, 377 (1990); P. Horava and E. Witten, Nucl. Phys. **B460**, 506 (1996); *ibid.* Nucl. Phys. **B475**, 94 (1996); E. Witten, Nucl. Phys. **471**, 135 (1996).
- [2] N. Arkani-Hamed, S. Dimopoulos and G. Dvali, Phys. Lett. **B429**, 263 (1998); I. Antoniadis *et al.*, Phys. Lett. **B436**, 257 (1998).
- [3] J. Lykken, Phys. Rev. **D54**, 3693 (1996); J. Dienes, E. Dudas and T. Ghergetta, Phys. Lett. **B436**, 55 (1998). G. Shiu and S.H. Tye, Phys. Rev. **D58**, 106007 (1998).
- [4] V. P. Mitrofanov and O. I. Ponomareva, Zh. Eksp. Teor. Fiz. **94**, 16 (1998) [Sov. Phys. JETP **67**, 1963 (1988)]; J. C. Long, H.W. Chan and J.C. Price, Nucl. Phys. **B539**, 23 (1999) and references therein.
- [5] G.F. Giudice, R. Rattazzi and J.D. Wells, Nucl. Phys. **B544**, 3 (1999).
- [6] T. Han, J.D. Lykken and R. Zhang, Phys. Rev. **D59**, 105006 (1999).
- [7] S. Nussinov and R. Shrock, Phys. Rev. **D59**, 105002 (1999); K. Cheung, Phys. Lett **B460**, 383 (1999); X.-G. He, Phys. Rev. **D** (to be published) hep-ph/9905500 (1999); T.G. Rizzo and J.D. Wells, Phys. Rev. **D** (to be published) hep-ph/9906234 (1999).
- [8] E.A. Mirabelli, M. Perelstein and M.E. Peskin, Phys. Rev. Lett. **82**, 2236 (1999); K. Cheung and W.-Y. Keung, Phys. Rev. **D60**, 112003 (1999); T. Han, D. Rainwater and D. Zeppenfeld, Phys. Lett. **B463**, 93 (1999).
- [9] D. Atwood, S. Bar-Shalom and A. Soni, hep-ph/9903538 and hep-ph/9909392 (1999).
- [10] J.L. Hewett, Phys. Rev. Lett. **82**, 4765 (1999); P. Mathews, S. Raychaudhuri and K. Sridhar, Phys. Lett. **B450**, 343 (1999); P. Mathews, S. Raychaudhuri and K. Sridhar, Phys. Lett. **B455**, 115 (1999); T.G. Rizzo, Phys. Rev. **D59**, 115010 (1999); K. Agashe and N.G. Deshpande, Phys. Lett. **B456**, 60 (1999); T.G. Rizzo, hep-ph/9902273 (1999); T. G. Rizzo, Phys. Rev. **D60**, 075001 (1999); P. Mathews, S. Raychaudhuri and K. Sridhar, hep-ph/9904232 (1999); A.K. Gupta, N.K. Mondal and S. Raychaudhuri, hep-ph/9904234 (1999); K.Y. Lee, H.S. Song and J.H. Song, Phys. Lett. **B464**, 82 (1999); X.-G. He, Phys. Rev. **D60**, 115017 (1999); P. Mathews, P. Poulose and K. Sridhar, Phys. Lett. **B461**, 196 (1999).

- [11] K. Cheung, Phys. Rev. **D** (to be published) hep-ph/9904266 (1999); H. Davoudiasl, Phys. Rev. **D60**, 084022 (1999).
- [12] T.G. Rizzo, Phys. Rev. **D60**, 115010 (1999).
- [13] See e.g., S. Dawson, Nucl. Phys. **B249**, 42 (1985); P.W. Johnson, F.I. Olness and W.-K. Tung, Phys. Rev. **D36**, 291 (1987); R.P. Kauffman, Phys. Rev. **D41**, 3343 (1990).
- [14] V. D. Barger and R. J. N. Phillips, *Collider Physics*, Addison-Wesley, Redwood City, CA (1987).
- [15] I. F. Ginzburg *et al.*, Nucl. Instrum. Methods. Phys. Res. **205**, 47 (1983); *ibid.* **A219**, 5 (1984).
- [16] J. F. Gunion, H. E. Haber, G. Kane and S. Dawson, *The Higgs Hunter's Guide*, Addison-Wesley, Redwood City, CA (1990).
- [17] H.L. Lai *et al.*, Phys. Rev. **bf D55**, 1280 (1997); H.L. Lai and W.K. Tung, Z. Phys. **C74**, 463 (1997), hep-ph/9701256; Also available in <http://www.phys.psu.edu/~cteq/>.
- [18] Notice that the lines in Fig. 7 end rather abruptly. This signifies that our 10 events criterion can not be met beyond the largest values of M_{VV}^{min} and/or M_{jj}^{min} shown. In these ranges of M_{VV}^{min} and/or M_{jj}^{min} we assume that no bound can be attained with a luminosity of $L = 30 \text{ fb}^{-1}$.